Chinese Chemical Letters 34 (2023) 108452

Contents lists available at ScienceDirect

Chinese Chemical Letters

journal homepage: www.elsevier.com/locate/cclet

Solvents/photo/pillar[5]arene triple responsive morphology and luminescence transformation from an amphiphilic dicyanostilbene-functionalized thiophene

Yang Wang[a,1], Haibo Zhong[a,b,1], Juan Yang[c,1], Yong Yao[a,*], Liang Li[b,*]

[a] School of Chemistry and Chemical Engineering, Nantong University, Nantong 226019, China
[b] School of Chemical and Environmental Engineering, Shanghai Institute of Technology, Shanghai 201418, China
[c] Nantong City Center for Disease Control and Prevention, Nantong 226019, China

ARTICLE INFO

Article history:
Received 21 February 2023
Revised 3 April 2023
Accepted 12 April 2023
Available online 14 April 2023

Keywords:
Pillar[5]arenes
Host-guest interactions
Amphiphilic
Self-assembly
Cell-imaging

ABSTRACT

α-Cyanostilbene (CS) based organic luminescent materials with efficient electrical conductivity, aggregation-induced enhanced emission, and controllable multi-colour emission properties, have been aroused wide attention by scientists over the past few years. Self-assembly of CS-motif in aqueous media refers to an environment-friendly method for preparing luminescent materials. However, it is still challenging to control the intrinsic hydrophobic properties of the organic components in aqueous media. In this study, an amphiphilic dicyanostilbene-functionalized thiophene (ACSTP) derivative was synthesized. *Z*-ACSTP was identified to dissolve in different organic solvents, accompanied with strong and tunable fluorescence emission. However, when *Z*-ACSTP was dispersed in water, it was self-assembled into nanofibers, and the fluorescence was red shifted, accompanied with sharp decrease of intensity compared with that in DMSO. Furthermore, *Z*-form of ACSTP to its *E*-form under 365 nm irradiation led to the morphology transformation from nanofibers to nanosheets. Notably, upon addition of water-soluble pillar[5]arene (WP5), the nanofibers were transformed into fluorescent hollow particles due to the host–guest interactions between the pyridinium group and WP5 and the obtained fluorescent particles can be further applied in living cell imaging.

Organic luminescent materials with controllable multi-colour emission have been aroused wide attention over the past few years for their promising applications in a wide variety of areas (*e.g.*, living cell imaging, light emitting diodes, molecular machines, visual displays, and optoelectronic devices) [1–5]. α-Cyanostilbene (CS) motifs have been confirmed as the significant building blocks for the construction of luminescent materials for their remarkable electrical and optical features (*e.g.*, efficient electrical conductivity, aggregation-induced enhanced emission, and controllable stimuli-responsive fluorescence) [6–8]. In this case, the luminescent materials fabricated by CS-motifs have dynamic and stimulation-responsive properties while exhibiting interesting optical properties [9–11]. On the other hand, the strategies based on self-assembly for designing multi-colour luminescent materials with great promise for their modular property and simpler synthetic routes. Moreover, the emitted colours can be modulated effectively using a wide variety of external stimuli (*e.g.*, solvent polarity, light irradiation, thermal stimulation, and humidity) [12–15]. Accordingly, self-assembly of CS-motif in aqueous media refers to an environment-friendly method for preparing luminescent materials [16–19]. However, it is still challenging to control the intrinsic hydrophobic properties of the organic components in aqueous media [20]. Host–guest interactions between organic building blocks and water-soluble macrocyclic host molecules have been confirmed as a successful strategy. After formation of the host-guest complex, the solubility, fluorescence, self-assembled morphology of the building blocks will change, while the resultant assemblies process stimuli-responsiveness [21–25]. For instance, Prof. Banerjee constructed tunable multi-colour luminescence successfully from the self-assembly of cyanostilbene⊃cucurbit[7]uril complex in water only by regulating the cyanostilbene/CB[7] ratio [22].

In this study, the fabrication of luminescent materials from the self-assembly of an amphiphilic dicyanostilbene-functionalized

* Corresponding authors.
E-mail addresses: yaoyong1986@ntu.edu.cn (Y. Yao), lilianglcx@sit.edu.cn (L. Li).
[1] These authors contributed equally to this work.

https://doi.org/10.1016/j.cclet.2023.108452
1001-8417/

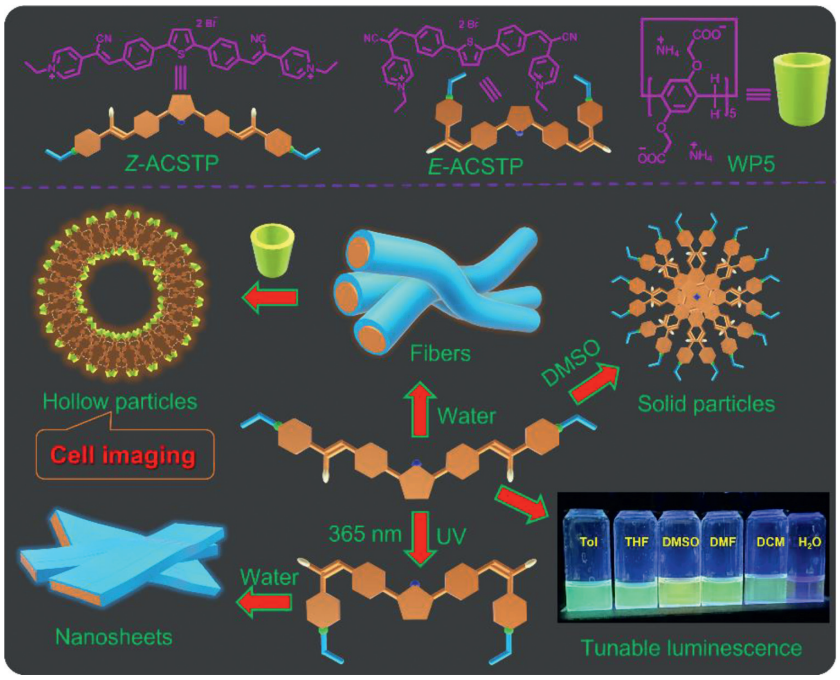

Scheme 1. Chemical structures of amphiphilic dicyanostilbene-functionalized thiophene (ACSTP) and the schematic illustration of the triple responsive morphology and luminescence transformation from ACSTP.

thiophene (ACSTP) derivative was reported (Scheme 1). *Z*-ACSTP was identified to dissolve in different organic solvents, accompanied with strong and tunable fluorescence emission. However, when *Z*-ACSTP was dispersed in water, it was self-assembled into nanofibers, and the fluorescence showed red shifted, accompanied with the sharp decrease of intensity compared with that in DMSO. Furthermore, the *Z*-form of ACSTP to its *E*-form under 365 nm irradiation led to morphology transformation from nanofibers to nanosheets. Notably, upon addition of water-soluble pillar[5]arene (WP5), the nanofibers were transformed into fluorescent hollow particles due to the host–guest interactions between the pyridinium group and WP5. The obtained fluorescent particles can be further applied to living cell imaging.

Z-ACSTP was prepared through three steps (Scheme S1 in Supporting information), and the structure of *Z*-ACSTP was characterized using ^{1}H NMR, ^{13}C NMR, and HR-ESI-MS technologies (Figs. S1–S3 in Supporting information). The as-prepared *Z*-ACSTP can dissolve into almost all organic solvents, and the obtained solution was highly stable. Besides, no aggregation was identified when the solution was left overnight (Fig. 1a, inset). UV–vis spectra indicated that the solutions of *Z*-ACSTP in DMSO, DMF, THF, DCM (CH_2Cl_2) or Tol (Toluene) showed the characteristic band of nearly 420 nm. However, when *Z*-ACSTP dissolved in CH_2Cl_2, the characteristic band was redshifted to 470 nm (Fig. 1a). Furthermore, all the solution exhibited bright fluorescence and the intensity variety from the polarity of the solvents (Fig. 1b).

The properties of *Z*-ACSTP in water/DMSO binary mixture were further investigated, and the water content in the system tended to be increased from 0% to 99%. The fluorescence emission peak was divided from 525 nm into two groups of peaks at 475 nm and 525 nm, respectively. With the increase of the water content, the emission peak at 475 nm tended to be decreased, while the peak at 525 nm gradually increased, indicating that there were two different assembly behaviours (Fig. 2a). When the water content was fixed at 99%, and the concentration of *Z*-ACSTP increased gradually, the result indicated that the peak at 425 nm continued to decline, whereas the peak at 575 nm was enhanced. Lastly, only the emission peak at 575 nm was observed, indicating that the assemblies were rearranged and formed a unique stable structure with the increase of the concentration (Fig. 2b). Subsequently, the morphology of the *Z*-ACSTP in DMSO/H_2O mixture was investigated according to SEM and TEM images. At the concentration of 10.0 mmol, the morphology of the assemblies transformed from nanoparticles with diameter about 70 nm (Fig. 2c; DMSO) to oblong-shaped nanoparticles (Fig. 2d; DMSO:H_2O = 1:99), as clearly depicted in the SEM images. However, the oblong-shaped nanoparticles in 99%

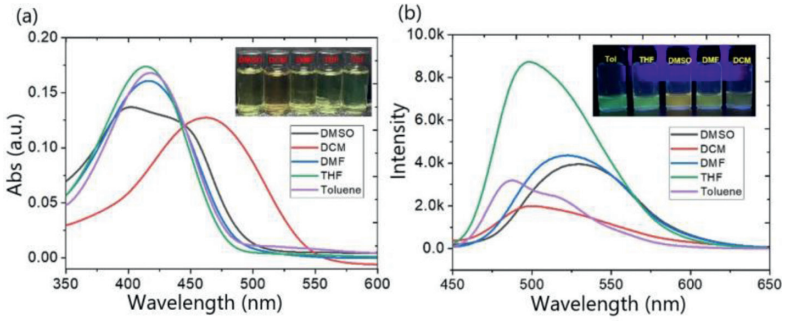

Fig. 1. (a) UV–vis absorption and (b) fluorescence emission spectra of *Z*-ACSTP (10 μmol/L) in different solvents. Inset: corresponding photo pictures.

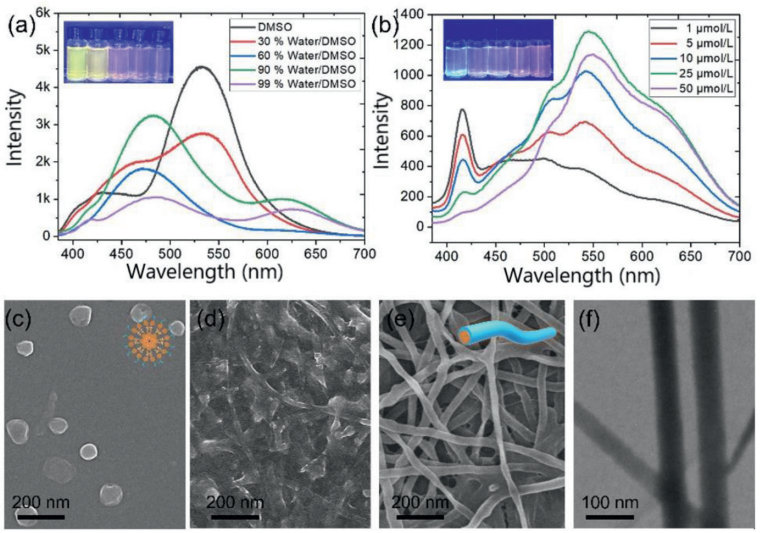

Fig. 2. (a) Fluorescence emission of *Z*-ACSTP (10 μmol/L) in different ratio of water/DMSO mixture. (b) Fluorescence emission spectra of *Z*-ACSTP with different concentration in 99% water/DMSO mixture. Inset: corresponding photo pictures. SEM image of *Z*-ACSTP (10 μmol/L) in DMSO (c) and in 99% water/DMSO mixture (d). SEM (e) and TEM (f) images of *Z*-ACSTP (50 μmol/L) in 99% water/DMSO mixture.

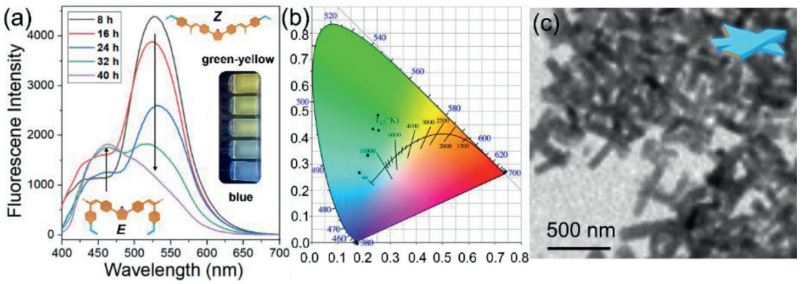

Fig. 3. (a) Fluorescence emission spectral changes of *Z*-ACSTP (10 μmol/L) upon different time photoirradiation in DMSO. Inset: the corresponding photo picture. (b) CIE 1931 diagram of *Z*-ACSTP under different UV irradiation time. (c) TEM image of *Z*-ACSTP (50 μmol/L) under 365 nm irradiation for 48 h in water.

water/DMSO mixture were further transformed into nanofibers with 50 nm in width and several micrometers in length (Figs. 2e and f) when the concentration was increased to 50.0 mmol, consisting with the fluorescence results.

It is generally known that the photoisomerization of cyanostilbene unit occurs from *Z*-to-*E* under 365 nm irradiation [26,27]. Compared to ^{1}H NMR spectrum of *Z*-ACSTP, several new peaks at δ 8.22, 8.19, 8.08, and 7.92 were observed, confirming the formation of *E*-ACSTP (Fig. S5 in Supporting information). The ESI-MS spectra of ACSTP showed no new peaks compared with the *Z*-isomers, suggesting that light irradiation did promote the *Z*-to-*E* isomerization of the part of cyanostilbene, rather than other types of photochemical reactions (Fig. S6 in Supporting information). Interestingly, the emission colour of *Z*-ACSTP in DMSO will be tunable with the change of illumination time. As shown in Fig. 3a, the initial excimeric emission peak in 525 nm decreased with a concomitant increase of emission in 475 nm (Fig. 3a), which was attributed to the formation of the corresponding *E*-ACSTP. Thus, the emission colour changed from green-yellow to blue by *in situ* photoirradiation (Fig. 3b). Furthermore, the morphology of the assemblies from *Z*-ACSTP in water also changed with 365 nm irradiation for 40 h. As shown in Fig. 3c, nanosheets with 70 nm in width and 360 nm in length were identified by SEM image, confirming the photo-induced morphology transformation.

Existing research has suggested that water-soluble pillar[5]arenes (WP5) modified with carboxylic groups can be associated with *N*-alkyl-pyridinium groups [28–31]. Since *Z*-ACSTP contains two *N*-alkyl-pyridinium groups, whether WP5 molecules can be complexed with *Z*-ACSTP and change the assemblies' morphology in water should be verified. First, after complexation, the H on pyridinium moved towards the higher field, indicating that the pyridinium group penetrated the cavity of WP5 (Fig. S7 in Supporting information). Second, the peaks at *m/z* 1892.69 and 955.36 were observed in the electrospray ionization mass spectrum (ESI-MS) of WP5/*Z*-ACSTP mixture (Fig. S8 in Supporting information), corresponding to $[(WP5)_2 + Z\text{-}ACSTP^{2+}\text{-}NH_4^+]^+$ and $[(WP5)_2 + Z\text{-}ACSTP^{2+}]^{2+}$, respectively, confirming the formation of $(WP5)_2 \supset Z$-ACSTP. Third, the FL intensity of *Z*-ACSTP was increased significantly through the addition of WP5. *Z*-ACSTP in the aqueous solution exhibited very weak fluorescence intensity (Fig. S9 in Supporting information). Upon addition WP5 gradually, the fluorescence intensity at approximately 475 nm was increased constantly. With the addition of WP5 twice, the fluorescence intensity of the system reached the maximum, nearly 4 times of the original *Z*-ACSTP. The reason for the above result is that the strong π–π stacking between *Z*-ACSTP molecules was inhibited after being complexing with two WP5 molecules. However, if WP5 was increased continuously, the fluorescence basically remained stable. Furthermore, the association constant (K_a) was determined as $(4.67 \pm 0.87) \times 10^4$ L/mol, and the stoichiometry between WP5 and *Z*-ACSTP was obtained as 2:1 through fluorescence titration (Fig. S10). Lastly, TEM and SEM images are beneficial to observe the new nanostructures after the addition of WP5 (Figs. 4b-d). As shown in Fig. 4b, hollow particles with an average diameter of

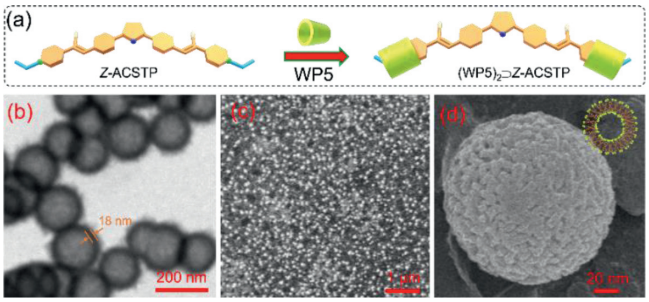

Fig. 4. (a) Schematic illustration of the formation of bola-amphiphilie $(WP5)_2\supset Z$-ACSTP. (b) TEM image of the hollow particles self-assembled from $(WP5)_2\supset Z$-ACSTP in water. (c) SEM and (d) enlarged SEM images of $(WP5)_2\supset Z$-ACSTP in water. $[C_{Z\text{-}ACSTP}] = 50$ μmol/L.

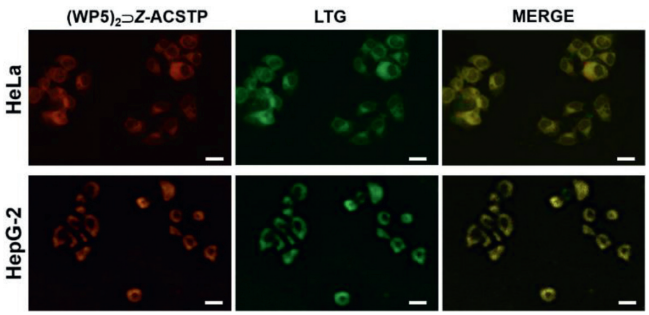

Fig. 5. Confocal laser scanning microscopy of HeLa and HepG2 cells after incubation with $(WP5)_2\supset Z$-ACSTP (5.00×10^{-4} mol/L) and Lyso-Tracker Green (LTG) for 4 h. Scale bar = 20 μm.

about 70 nm are observed. The thickness of the hollow vesicle was determined as be 18 nm (Fig. 4b), larger than the extending length of $(WP5)_2\supset Z$-ACSTP, indicating the vesicles with multi-layer walls.

Furthermore, a question was raised about whether such $(WP5)_2\supset Z$-ACSTP based hollow particles can apply to biomedicine associated fields. Accordingly, the cellular imaging properties of the hollow particles were examined. At first, the cytotoxicity of $(WP5)_2\supset Z$-ACSTP based hollow particles have been evaluated. Human cervical carcinoma (HeLa) cells were incubated with $(WP5)_2\supset Z$-ACSTP at concentrations ranging from 5.0 μg/mL to 80 μg/mL for 4 h, the viability of HeLa cells was basically unchanged by 3-(4,5-dimethylthiazol-2-yl)-2,5-diphenyltetra-zolium bromide (MTT) assays, indicating the good cellular compatibility and low cytotoxicity of $(WP5)_2\supset Z$-ACSTP-based particles (Fig. S11 in Supporting information) [32]. Subsequently, HeLa and hepatocellular carcinoma (HepG2) cells were chosen to be administrated with $(WP5)_2\supset Z$-ACSTP for 4 h. Next, the intracellular distribution of the $(WP5)_2\supset Z$-ACSTP based assemblies was determined under confocal laser scanning microscopy (CLSM). As shown in Fig. 5, both HeLa and HepG2 cells treated with $(WP5)_2\supset Z$-ACSTP exhibited strong red fluorescence in the cytoplasm of the cells. To further study the subcellular distribution of $(WP5)_2\supset Z$-ACSTP-based hollow particles, the cells were *co*-stained with $(WP5)_2\supset Z$-ACSTP and commercially available lysosome staining dye Lyso-Tracker Green (LTG). Under the effect of the merged orange dyeing site of red $(WP5)_2\supset Z$-ACSTP and green LTG, $(WP5)_2\supset Z$-ACSTP and LTG were in favourable co-localization. The above results provide a convenient pathway for co-staining lysosomes in living cells due to the high coincidence of stained position between $(WP5)_2\supset Z$-ACSTP and LTG [33,34].

In conclusion, an amphiphilic dicyanostilbene-functionalized thiophene (ACSTP) was designed and synthesized. *Z*-ACSTP exhibited strong fluorescence when dissolving into a wide variety of organic solvents. However, with the increase of the water content in DMSO, the fluorescence intensity was decreased, and the morphology of the assemblies changed from nanoparticles in DMSO to nanofiber in water. It is noteworthy that 365 nm UV light induced *Z*-to-*E* photoisomerization of the cyanostilbene unit led to the change of emission colour from green-yellow to blue and the morphology from nanofibers to nanosheets. Besides, under the effect of the host–guest interactions between the pyridinium group and WP5, the nanofibers from *Z*-ACSTP in water was transformed into fluorescent hollow particles through the addition of WP5, which can be further applied in living cell imaging. This study suggests that the present results of this study provide a reference for designing intelligent systems with luminescent colour and morphology tuning properties for potential applications in bioluminescence detection.

Declaration of competing interest

The authors declare that they have no known competing financial interests or personal relationships that could have appeared to influence the work reported in this paper.

Acknowledgments

This work was supported by the National Natural Science Foundation of China (Nos. 21801139, 32101215, 22007052), Natural Science Foundation of Jiangsu Province (Nos. BK20180942, BK20190917). We also thank Nantong University Analysis & Testing center for characterization.

Supplementary materials

Supplementary material associated with this article can be found, in the online version, at doi:10.1016/j.cclet.2023.108452.

References

[1] F. Li, M. Wang, S. Liu, Q. Zhao, Chem. Sci. 13 (2022) 2184–2201.
[2] S. Chen, X.-D. Wang, M.-P. Zhuo, et al., Sci. China Chem. 65 (2022) 740–745.
[3] G. Jiang, J. Yu, J. Wang, B.Z. Tang, Aggregate 3 (2022) e285.
[4] Y. Wang, H. Wu, W. Hu, J.F. Stoddart, Adv. Mater. 34 (2022) 2105405.
[5] R. Chen, Y. Guan, H. Wang, et al., ACS Appl. Mater. Interfaces 13 (2021) 41131–41139.
[6] M. Martínez-Abadía, R. Giménez, M.B. Ros, Adv. Mater. 30 (2018) 1704161.
[7] S.K. Bhaumik, S. Banerjee, Chem. Commun. 56 (2020) 655–658.
[8] J. Wang, P. Li, C. Ji, et al., J. Mater. Chem. C 10 (2022) 15145–15151.
[9] W. Fang, W. Zhao, P. Pei, et al., J. Mater. Chem. C 6 (2018) 9269–9276.
[10] X. Jin, D. Yang, Y. Jiang, P. Duan, M. Liu, Chem. Commun. 54 (2018) 4513–4516.
[11] L. Ma, R. Tang, Y. Zhou, et al., Chem. Commun. 58 (2022) 8978–8981.
[12] H. Zhong, L. Li, S. Zhu, Y. Wang, Front. Chem. 10 (2022) 980173.
[13] Y. Ren, R. Zhang, C. Yan, et al., Tetrahedron 73 (2017) 5253–5259.
[14] J. Liao, M. Yang, Z. Liu, H. Zhang, J. Mater. Chem. A 7 (2019) 2002–2008.
[15] G. Hou, S. Min, Y. Zhao, et al., Dye. Pigments 180 (2020) 108460.
[16] S.K. Bhaumik, S. Banerjee, ACS Appl. Mater. Interfaces 14 (2022) 36936–36946.
[17] G. Sun, W. Qian, J. Jiao, et al., J. Mater. Chem. A 8 (2020) 9590–9596.
[18] K. Diao, D.J. Whitaker, Z. Huang, et al., Chem. Commun. 58 (2022) 2343–2346.
[19] T. Xiao, L. Tang, D. Ren, Chem. Eur. J. 29 (2023) e202203463.
[20] J. Seo, J.W. Chung, J.E. Kwona, S.Y. Park, Chem. Sci. 5 (2014) 4845–4850.
[21] H. Guo, X. Yan, B. Lu, et al., J. Mater. Chem. C 8 (2020) 15622–15625.
[22] M. Yamashina, M.M. Sartin, Y. Sei, et al., J. Am. Chem. Soc. 137 (2015) 9266–9269.
[23] E. Li, K. Jie, Y. Zhou, R. Zhao, F. Huang, J. Am. Chem. Soc. 140 (2018) 15070–15079.
[24] Y. Li, Y. Dong, X. Miao, et al., Angew. Chem. Int. Ed. 57 (2018) 729–733.
[25] H. Yang, Y. Liu, K. Liu, et al., Langmuir 29 (2013) 12909–12914.
[26] L. Zhu, X. Li, Q. Zhang, et al., J. Am. Chem. Soc. 135 (2013) 5175–5182.
[27] J. Liu, W. Li, M. Liu, et al., Phys. Chem. Chem. Phys. 20 (2018) 28279–28286.
[28] J. Wang, M. Cen, J. Wang, et al., Chin. Chem. Lett. 33 (2022) 1475–1478.
[29] D. Xia, P. Wang, B. Shi, Org. Lett. 19 (2017) 202–205.
[30] T. Ogoshi, M. Hashizume, T. Yamagishia, Y. Nakamoto, Chem. Commun. 46 (2010) 3708–3710.
[31] X. Lv, D. Xia, Y. Zuo, et al., Langmuir 35 (2019) 8383–8388.
[32] Y. Jiao, S. Lan, D. Ma, Chin. Chem. Lett. 32 (2021) 1025–1028.
[33] X.K. Ma, Y.M. Zhang, Q. Yu, et al., Chem. Commun. 57 (2021) 1214–1217.
[34] Q. Wang, J. Fan, X. Bian, et al., Chin. Chem. Lett. 33 (2022) 1979–1982.